

# IMPLEMENTATION OF A HOMOGENEOUS HIGH-SHEET-RESISTANCE EMITTER IN MULTICRYSTALLINE SILICON SOLAR CELLS

Vijay Yelundur, Kenta Nakayashiki, Mohamed Hilali, Ajeet Rohatgi  
University Center of Excellence for Photovoltaics Research and Education, School of Electrical and Computer Engineering, Georgia Institute of Technology, 777 Atlantic Dr. Atlanta, GA 30332-0250

## ABSTRACT

Solar cell efficiency enhancement resulting from the implementation of a high-sheet-resistance emitter (95  $\Omega/\text{sq.}$ ) in multicrystalline silicon solar cells with screen-printed contacts is demonstrated in this paper. Solar cells on low-cost String Ribbon Si from Evergreen Solar, Baysix mc-Si from Deutsche Solar, and high-quality float zone silicon with 45  $\Omega/\text{sq.}$  and 95  $\Omega/\text{sq.}$  phosphorus-doped  $n^+$ -emitters are fabricated with RTP-fired screen-printed contacts and characterized to assess the impact of a high-emitter-sheet resistance emitter on cell performance. Screen-printed mc-Si solar cells show an improvement in  $V_{oc}$  of 4-5 mV in most cases that is attributed to the use of the high-sheet-resistance emitter. An appreciable increase in  $J_{sc}$  by as much as 1.0  $\text{mA}/\text{cm}^2$  is also observed due to enhanced blue response identified by internal quantum efficiency measurement.

## INTRODUCTION

Most industrial multicrystalline silicon solar cells are fabricated with a phosphorus-doped  $n^+$ -emitter layer having a sheet resistance of 40-50  $\Omega/\text{sq.}$ . The relatively low sheet resistance in conventional mc-Si cells is chosen to promote a low-resistance ohmic contact between the screen-printed metallization and the emitter layer. However the heavy doping increases carrier recombination in the emitter layer [1] and increases the emitter surface recombination velocity [2]. An improvement to solar cell efficiency can be achieved if the emitter doping can be reduced to minimize recombination, without degrading the fill factor. A recent study has shown that the  $J_{sc}$  and  $V_{oc}$  of mc-Si solar cells can be increased if the emitter sheet resistance is increased [3]. However, degradation of the FF limited the maximum sheet resistance to 70  $\Omega/\text{sq.}$  for optimal cell performance. High-quality screen-printed solar cells have been achieved recently on even higher sheet-resistance emitters (100  $\Omega/\text{sq.}$ ) by Hilali et al. [4] on single crystal Si. Through appropriate selection and optimization of the Ag paste, firing recipe, emitter surface passivation and grid design, the authors achieved an efficiency of 17.4%.

In this paper, we investigate the impact of the high-sheet-resistance emitter on solar cells using low-cost mc-Si materials. In these materials, relatively low bulk carrier lifetimes are expected to increase base component of the reverse saturation current density ( $J_{ob}$ ), and hence the

total  $J_o$ , if significant lifetime enhancement does not occur during cell processing. Thus lifetime enhancement is crucial to realizing an improvement in the  $V_{oc}$  when a high sheet resistance emitter is applied to mc-Si solar cells. Our work has shown that proper implementation of rapid thermal firing (RTF) of screen-printed contacts can lead to a minority carrier lifetime enhancement from 3  $\mu\text{s}$  to 90  $\mu\text{s}$  or greater [5], which should significantly reduce  $J_{ob}$ . The objective of this paper is to characterize the efficiency enhancement, if any, due to the implementation of a high-sheet-resistance emitter in multicrystalline silicon solar cells with screen-printed contacts. Solar cells on low-cost String Ribbon Si from Evergreen Solar, Baysix mc-Si from Deutsche Solar, and high-quality float zone silicon with high- and low-sheet-resistance emitters are fabricated and characterized to assess the impact of a high-sheet-resistance emitter on  $V_{oc}$ ,  $J_{sc}$ , and FF. Device simulations are performed to support the experimental results.

## EXPERIMENTAL

The  $J_{oe}$  for 45 and 95  $\Omega/\text{sq.}$  emitters was measured on 500  $\Omega\text{-cm}$  n-type float zone Si wafers after  $\text{POCl}_3$  diffusion and PECVD  $\text{SiN}_x$  deposition on both sides. The 45  $\Omega/\text{sq.}$  diffusion was performed at 874°C and had a surface concentration of  $2.3 \times 10^{20} \text{ cm}^{-3}$  and a junction depth of 0.5  $\mu\text{m}$ , while the 95  $\Omega/\text{sq.}$  diffusion was performed at 850°C and had a surface concentration of  $1.7 \times 10^{17} \text{ cm}^{-3}$  and a junction depth of 0.3  $\mu\text{m}$ . The  $\text{SiN}$  layers with a thickness of 80 nm and an index of refraction of 2.0 were deposited on both wafer surfaces in a horizontal tube direct PECVD system operating at a frequency of 50 kHz and a temperature of 425°C.  $J_{oe}$  was measured by the transient photoconductance decay method before and after RTP firing using the WCT-100 tool from Sinton Consulting. Then wafers were subjected to the RTF process without screen-printed metallization and measured again to determine the  $J_{oe}$  after cell processing. The minority carrier lifetime was monitored in mc-Si wafers by the quasi steady state photoconductance (QSSPC) technique before and after solar cell processing. The lifetime was measured on eight points of three wafers for each mc-Si material before processing, after emitter diffusion, and after cell processing at an excess carrier concentration of  $1 \times 10^{15} \text{ cm}^{-3}$ . Screen-printed  $n^+$ -p-p<sup>+</sup> solar cells were fabricated on 1.3  $\Omega\text{-cm}$  float zone Si, 1.5  $\Omega\text{-cm}$  Baysix mc-Si, and  $\sim 3$   $\Omega\text{-cm}$  String Ribbon Si. Phosphorus diffusion for 45 and 95  $\Omega/\text{sq.}$  emitters was

performed using a liquid  $\text{POCl}_3$  source as described above. After removal of the phosphorus glass, the  $\text{SiN}_x$  layer was deposited on the front surface of all wafers and commercially available Al and Ag pastes from Ferro Corp. were screen printed on to the rear and front of all samples, respectively. A grid specifically optimized for high-sheet-resistance emitters [4] was used for cells with a  $95 \Omega/\text{sq}$  emitter. All solar cells were co-fired using RTF with the same firing recipe and peak temperature. Cells were isolated using a dicing saw to define an active area of  $4 \text{ cm}^2$ , and annealed in forming gas at  $400^\circ\text{C}$  for 10 minutes.

## RESULTS

### Effect of the emitter saturation current density for high- and low-sheet-resistance emitters on the $V_{oc}$ of mc-Si cells

Figure 1 shows the  $J_{oe}$  for  $45 \Omega/\text{sq}$ . and  $95 \Omega/\text{sq}$ . emitters coated with  $\text{SiN}_x$  before and after RTP firing. The  $J_{oe}$  after  $\text{SiN}_x$  deposition was  $456 \text{ fA/cm}^2$  for the  $45 \Omega/\text{sq}$ . emitter and  $447 \text{ fA/cm}^2$  for the  $95 \Omega/\text{sq}$ . emitter. The  $J_{oe}$  values decreased to 187 and  $107 \text{ fA/cm}^2$  for 45 and  $95 \Omega/\text{sq}$ . emitters, respectively after RTF without screen-printed metallization. The decrease of  $J_{oe}$  for both 45 and  $95 \Omega/\text{sq}$ . emitters after RTF is attributed to the alleviation of surface damage that was caused by ion bombardment of the surface during low-frequency PECVD  $\text{SiN}_x$  deposition. PC1D simulations were performed to predict the impact of the measured  $J_{oe}$  values for high- and low-sheet-resistance emitters on  $V_{oc}$  for solar cells with high and low bulk minority carrier lifetime. In these simulations,  $J_{oe}$  values of 187 and  $107 \text{ fA/cm}^2$  were used for 45 and  $95 \Omega/\text{sq}$ . emitters, respectively, and a back surface recombination velocity of  $500 \text{ cm/s}$  and base resistivity of  $1 \Omega\text{-cm}$  were assumed. The results shown in Fig. 2 demonstrate that a high sheet resistance emitter will not

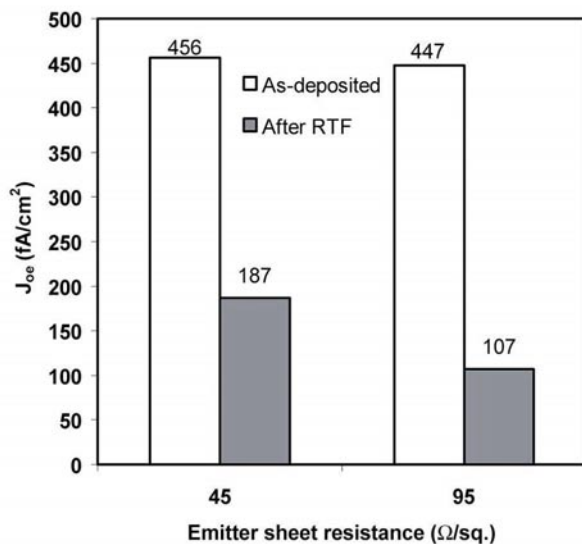


Fig. 1.  $J_{oe}$  of 45 and  $95 \Omega/\text{sq}$ . emitters before and after RTF.

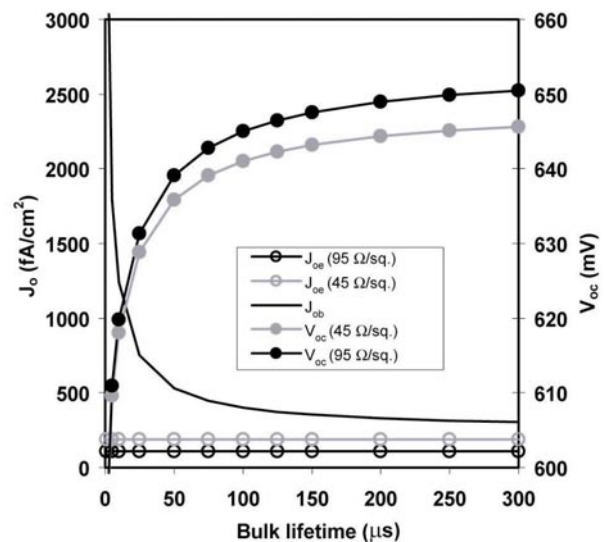


Fig. 2 Simulation of the improvement of  $V_{oc}$  from a high-sheet-resistance emitter as a function of bulk lifetime for a base resistivity of  $1 \Omega\text{-cm}$ .

significant increase the  $V_{oc}$  of low-lifetime solar cells. When the bulk lifetime is  $25 \mu\text{s}$ ,  $J_{ob}$  dominates  $V_{oc}$  and replacement of the  $45 \Omega/\text{sq}$ . emitter with a  $95 \Omega/\text{sq}$ . improves  $V_{oc}$  by only 2 mV. As the bulk lifetime increases,  $J_{ob}$  decreases and the effect of the high-sheet-resistance emitter on  $V_{oc}$  becomes more significant. For example, when the bulk lifetime increases to  $75 \mu\text{s}$ , the high-sheet-resistance emitter improves  $V_{oc}$  by 4 mV. This result indicates that lifetime enhancement is crucial to realizing an improvement in the  $V_{oc}$  when a high-sheet-resistance emitter is applied to mc-Si solar cells.

The average carrier lifetime in Baysix, EFG, and String Ribbon was measured to determine if the post-processing lifetime reaches  $75 \mu\text{s}$  and appreciable  $V_{oc}$  enhancement can be achieved. Figure 3 shows that phosphorus gettering during emitter diffusion increases

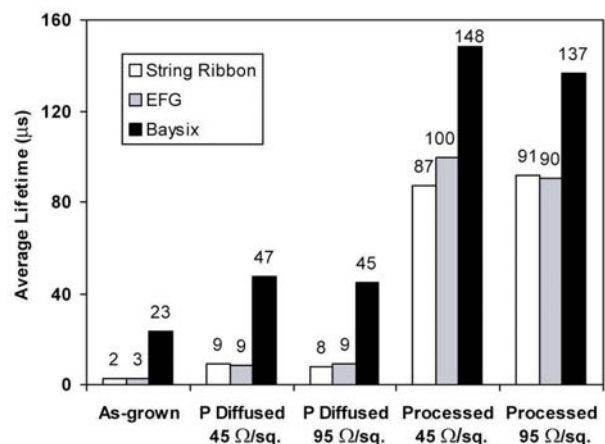


Fig. 3. Average lifetime in Baysix, EFG, and String Ribbon Si measured before and after cell processing for high- and low-sheet-resistance emitters.

the average lifetime to from about 2  $\mu$ s to 8  $\mu$ s for EFG and String Ribbon Si and from 23  $\mu$ s to about 45  $\mu$ s. Note that the emitter sheet resistance, controlled by the diffusion temperature, does not strongly effect this lifetime enhancement. Figure 3 also shows that the average lifetime in these materials increases to about 90 to 150  $\mu$ s after cell processing, which included phosphorus diffusion, SiN<sub>x</sub> deposition, screen-printing, and RTF. According to the device simulations in Fig. 2, these lifetime values are high enough to realize a V<sub>oc</sub> enhancement when a high-sheet- resistance emitter is applied.

### Enhancement of mc-Si solar cell performance through implementation of a homogenous high sheet resistance emitter

A summary of the average performance and the best cells fabricated on float zone, Baysix, EFG, and String Ribbon Si with 45 and 95  $\Omega$ /sq. emitters are shown in Table 1. A total 17 to 34 cells were made in each case. The data shows that the high sheet resistance emitter improves the average cell efficiency by as much as 0.5% absolute without severely degrading the FF. A V<sub>oc</sub> and J<sub>sc</sub> enhancement attributed to the high-sheet-resistance emitter was obtained for each material, while the average FF decreased slightly. For float zone, Baysix mc-Si, and EFG cells, the average V<sub>oc</sub> increased by 4-5 mV when the 95  $\Omega$ /sq. emitter was applied. This improvement in V<sub>oc</sub> is in good agreement with the device simulations shown in Fig. 2. However, the V<sub>oc</sub> enhancement achieved in String Ribbon cells (8 mV) was slightly in excess of that predicted by PC1D simulations and may be caused by the

Table 1. Average performance and best results for 4 cm<sup>2</sup> solar cells with high sheet resistance emitters.

Material	Emitter $\Omega$ /sq	V <sub>oc</sub> (mV)	J <sub>sc</sub> (mA/cm <sup>2</sup> )	FF	Eff. (%)
Float Zone	45	631	34.3	0.762	16.5
	95	636	35.2	0.755	16.9
	95 best cell	640	35.4	0.769	17.4
Baysix	45	616	32.7	0.774	15.6
	95	620	33.0	0.768	15.7
	95 best cell	628	33.6	0.780	16.2
EFG	45	596	33.2	0.766	15.2
	95	601	33.5	0.758	15.3
	95 best cell	610	33.0	0.778	15.6
String Ribbon	45	595	31.9	0.774	14.7
	95	603	32.9	0.766	15.2
	95 best cell	611	34.2	0.774	16.2

limited number of samples processed in this study. Float zone and String Ribbon solar cells showed a significant improvement in J<sub>sc</sub> by about 1.0 mA/cm<sup>2</sup> due to the use of the high-sheet-resistance emitter. This improvement is identified in the short wavelength IQE for float zone and String Ribbon cells shown in Fig. 3. PC1D simulations of the measured IQE data showed that the front surface recombination velocity (FSRV) in float zone and String Ribbon Si cells reduces by a factor of approximately two when the 45  $\Omega$ /sq. emitter is replaced with the 95  $\Omega$ /sq. emitter. The enhanced J<sub>sc</sub> and V<sub>oc</sub> from the

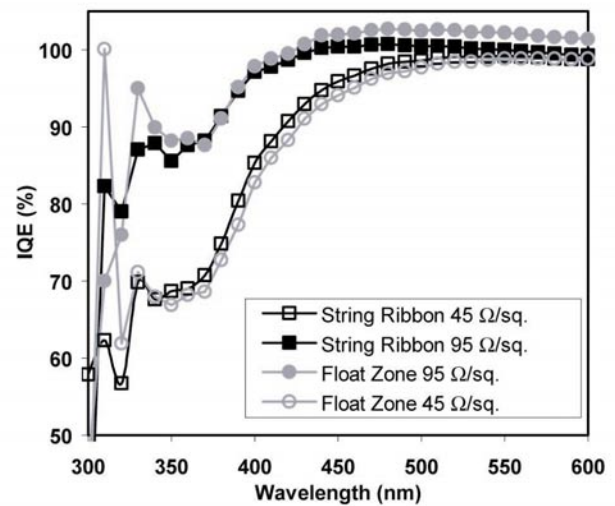


Fig. 4 Short wavelength IQE of float zone and String Ribbon cells with 45 and 95  $\Omega$ /sq. emitters.

implementation of the homogenous high-sheet-resistance emitter resulted in maximum cell efficiencies of 17.4% on float zone Si, 16.2% on Baysix mc-Si, 15.6% on EFG Si, and 16.2% on String Ribbon Si as shown in Table 1. The I-V data for the 16.2%-efficient String Ribbon cell under illumination measured at NREL is shown in Fig. 5. This is the highest reported efficiency for String Ribbon solar cells with screen-printed contacts and a single-layer antireflection coating.

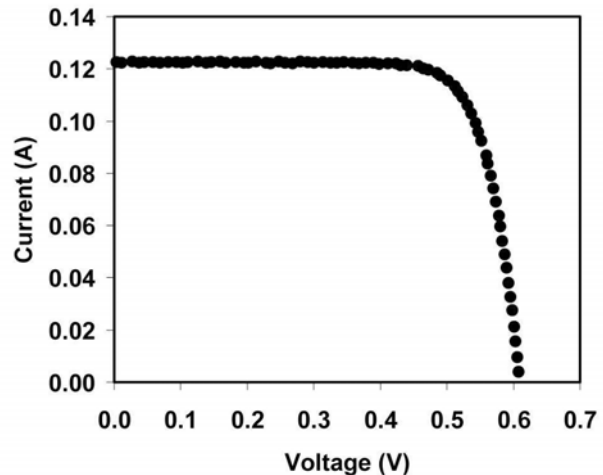


Fig. 5 I-V data under illumination for the 16.2% - efficient String Ribbon Si solar cell with a 95  $\Omega$ /sq. emitter measured by NREL.

### CONCLUSIONS

Solar cell efficiency enhancement of 0.1 to 0.5% absolute resulted from the implementation of a high-sheet-resistance emitter (95  $\Omega$ /sq.) with RTP-fired screen-printed

contacts in silicon solar cells on low-cost String Ribbon Si from Evergreen Solar, Baysix mc-Si from Deutsche Solar, and high-quality float zone silicon.  $J_{oe}$  values of 187 and 107  $\text{fA/cm}^2$  for 45 and 95  $\Omega/\text{sq}$ . emitters respectively were measured after low-frequency PECVD SiN deposition and RTF.  $V_{oc}$  enhancement by 4-5 mV was predicted based on the measured  $J_{oe}$  values and device simulations for solar cells with bulk lifetimes of 75  $\mu\text{s}$  or higher. This enhancement was experimentally observed along with an increase in  $J_{sc}$  by as much as 1.0  $\text{mA/cm}^2$ . The increase in  $J_{sc}$  primarily due to enhanced blue response identified by IQE measurement. Analysis of the IQE showed that the lightly doped emitter lowers the FSRV in String Ribbon and float zone cells by a factor of approximately two. The enhanced  $J_{sc}$  and  $V_{oc}$  from the implementation of the homogenous high-sheet-resistance emitter resulted in maximum cell efficiencies of 17.4% on float zone Si, 16.2% on Baysix mc-Si, 15.6% on EFG Si, and 16.2% on String Ribbon Si. Further process optimization is expected to improve the fill factor in high-sheet-resistance emitter cells from 0.76 to  $\geq 0.77$ , and result in mc-Si cell efficiencies in the range of 16% to 17%.

## REFERENCES

- [1] A. Cuevas and D. Russell, "Co-optimisation of the emitter region and the metal grid of silicon solar cells," *Prog. Photovolt.: Res. Appl.*, 8, 1999, pp. 603-616.
- [2] M. Kerr et al., "Surface recombination velocity of phosphorus-diffused silicon solar cell emitters passivated with plasma enhanced chemical vapor deposited silicon nitride and thermal silicon oxide," *J. Appl. Phys.*, 89, 2001, pp. 3821-3826.
- [3] M. Bähr et al., "Surface passivation and contact resistance on various emitters of screen-printed crystalline solar cells," Nineteenth EUPVSEC, 2004 (at press).
- [4] M Hilali et al., "Development of screen-printed Si solar cells with high fill factors on 100  $\Omega/\text{sq}$  emitters," *IEEE Trans. Electron Dev.* 51, 2004, pp. 948-955.
- [5] K. Nakayashiki et al., "Minority-carrier lifetime enhancement in edge-defined film-fed grown Si through rapid thermal processing-assisted reduction," pp. 97-104.